

Direct impact of climate change on groundwater levels in the Iberian Peninsula

Amir Rouhani^{1,*}, Nahed Ben-Salem¹, Marco D'Oria², Rafael Chávez García Silva¹, Alberto Viglione³, Nadim K. Copty⁴, Michael Rode^{1,5}, David Andrew Barry⁶, J. Jaime Gómez-Hernández⁷, Seifeddine Jomaa¹

¹Department of Aquatic Ecosystem Analysis and Management, Helmholtz Centre for Environmental Research - UFZ, Magdeburg, Germany (amir.rouhani@ufz.de, nahed.ben-salem@ufz.de, rafael.chavez@ufz.de, michael.rode@ufz.de, seifeddine.jomaa@ufz.de)

²Department of Engineering and Architecture, University of Parma, Parma, Italy (marco.doria@unipr.it)

³Department of Environment, Land and Infrastructure Engineering, Polytechnic of Turin, Turin, Italy (alberto.viglione@polito.it)

⁴Institute of Environmental Sciences, Boğaziçi University, Istanbul, Türkiye (ncopty@bogazici.edu.tr)

⁵Institute for Environmental Science and Geography, University of Potsdam, Potsdam, Germany

⁶Ecological Engineering Laboratory (ECOL), Environmental Engineering Institute (IIE), Faculty of Architecture, Civil and Environmental Engineering (ENAC), École Polytechnique Fédérale de Lausanne (EPFL), Lausanne, Switzerland. (andrew.barry@epfl.ch)

⁷Institute of Water and Environmental Engineering, Universitat Politècnica de València, Valencia, Spain (jaime@dihma.upv.es)

*Corresponding author (amir.rouhani@ufz.de)

Correction Notice: This is the accepted manuscript with the Figures in the correct order, which unfortunately were shuffled around in the published online version available at [Science of the Total Environment Journal](https://doi.org/10.1016/j.scitotenv.2025.179009) making it difficult to read.

Accepted in *Science of the Total Environment Journal*, (26 February 2025)

<https://doi.org/10.1016/j.scitotenv.2025.179009>

1 Abstract

2 The Iberian Peninsula is a water-scarce region that is increasingly reliant on groundwater. Climate
3 change is expected to exacerbate this situation due to projected irregular precipitation patterns and
4 frequent droughts. Here, we utilised convolutional neural networks (CNNs) to assess the direct effect
5 of climate change on groundwater levels, using monthly meteorological data and historical
6 groundwater levels from 3829 wells. We considered temperature and antecedent cumulative
7 precipitation over 3, 6, 12, 18, 24, and 36 months to account for the recharge time lag between
8 precipitation and groundwater level changes. Based on CNN performance, 92 location-specific
9 models were retained for further analysis, representing wells spatially distributed throughout the
10 peninsula. The CNNs were used to assess the influence of climate change on future groundwater
11 levels, considering an ensemble of eight combinations of general and regional climate models under
12 the RCP4.5 and RCP8.5 scenarios. Under RCP4.5, an average annual temperature increase of
13 1.7°C and a 5.2% decrease in annual precipitation will result in approximately 15% of wells
14 experiencing > 1-m decline between the reference period [1986-2005] and the long-term period
15 [2080-2100]. Under RCP8.5, with a 3.8°C increase in temperature and a 20.2% decrease in annual
16 precipitation between the same time periods, 40% of wells are expected to experience a water level
17 drop of > 1 m. Notably, for 72% of the wells, temperature is the main driver, implying that evaporation
18 has a greater impact on groundwater levels. Effective management strategies should be
19 implemented to limit overexploitation of groundwater reserves and improve resilience to future
20 climate changes.

21 Keywords

22 water table depth, groundwater management, water scarcity, Mediterranean, groundwater
23 sustainability, convolutional neural networks
24

25 Highlights

- 26 • Data-driven assessment of climate change on groundwater in the Iberian Peninsula
- 27 • Deep learning (CNN) was used to create site-specific groundwater models
- 28 • Evaporation has a major influence on shallow groundwater levels
- 29 • Resilient groundwater management essential to mitigate climate change impacts

30 1. Introduction

31 Groundwater accounts for 99% of the planet's total liquid fresh water, serving as a strategic resource
32 for multiple sectors, including drinking water, agriculture, and ecosystem services. Groundwater is
33 the main source of fresh water for more than two billion people worldwide (Adams et al., 2022; Alley
34 et al., 2002; Gleeson et al., 2012), making up more than 20% of global water usage and 43% of
35 irrigation water (Earman and Dettinger, 2011; Zektser and Everett, 2004). With continued growth of
36 the global population and projected changing climate, it is anticipated that groundwater's contribution
37 will rise as surface water resources become less dependable (Adams et al., 2022; Burchi and
38 Mechlem, 2005; UN World Water Development Report., 2020)).

39 In the Iberian Peninsula, groundwater plays a vital role in supporting domestic and agricultural
40 needs. Spain relies on an estimated 131 m³ of annual per capita extraction, with 30 m³ used for
41 domestic purposes and 94 m³ for irrigation, while Portugal exhibits one of the highest global
42 extraction rates at 474 m³ per capita, including 33 m³ for domestic use and over 420 m³ for irrigation
43 (Margat and Gun, 2013). Groundwater has sustained essential water supplies, such as Porto's
44 Paranhos spring system, in use since 1120 AD (Chaminé et al., 2010). The region's agri-food sector

45 is critical to Europe's food security, with exports of olive oil, wine, and fresh products valued at €15
46 billion in 2022 (Eurostat and Cook, 2024; Moral-Pajares et al., 2024). These factors underscore the
47 need for sustainable groundwater management amidst growing environmental challenges.

48 The hydrogeological conditions of the Iberian Peninsula are shaped by its diverse geological
49 formations, variable climate, and historical fluctuations in precipitation and temperature.
50 Groundwater is a vital resource for ecosystems, agriculture, and domestic supply in the region, with
51 aquifers playing a crucial role in storing and regulating water. The peninsula features both shallow
52 and deep aquifers, with shallow systems averaging 36 m in depth, making them particularly
53 vulnerable to climatic variability. Deeper aquifers, often semi-confined, provide more stable
54 freshwater reserves, capable of buffering against short-term climatic changes. However, they are
55 susceptible to long-term anthropogenic and climatic pressures (Diodato et al., 2024; Estrela et al.,
56 2024).

57 The geological diversity of the peninsula includes porous, fractured, and karstic aquifer systems,
58 each with distinct hydrogeological properties. In regions like Castile and León, the aquifer system
59 consists of an unconfined upper layer and a semi-confined deeper layer, forming a complex 3D
60 network. Recharge in these systems primarily occurs through meteoric infiltration, with rivers such
61 as the Duero acting as major discharge outlets. Karstic aquifers, characterized by high permeability
62 due to dissolution features in limestone and dolomitic formations, are critical for water storage and
63 flow. These systems are particularly sensitive to variations in precipitation and anthropogenic
64 extraction, which influence their recharge and discharge dynamics. Extensive groundwater pumping
65 in many areas, such as Castile and León, has led to significant declines in water table levels,
66 highlighting the challenges of balancing extraction with natural replenishment (Diodato et al., 2024;
67 García-Valdecasas Ojeda et al., 2021).

68 The interplay of geological diversity, shallow aquifer vulnerability, and climatic variability
69 underscores the complexity of groundwater dynamics in the Iberian Peninsula. Sustainable
70 management efforts must account for the unique geological characteristics of these aquifers, along
71 with their sensitivity to climatic influences, to ensure the resilience of water systems that are critical
72 for the region's ecosystems and human livelihoods (Estrela et al., 2024; García-Valdecasas Ojeda
73 et al., 2021). Recent studies highlighted the increasing stress on groundwater resources caused by
74 climate change, heatwaves, and human activity, affecting both groundwater quantity and quality.
75 Due to climate change and water scarcity, Catalonia in the western Mediterranean region of the
76 Iberian Peninsula is experiencing a severe drought and increased groundwater nitrate pollution
77 (Mas-Pla and Menció, 2019). Groundwater in the peninsula is also important for various ecosystems,
78 particularly in the Mediterranean area. Groundwater uptake predominates during the dry summer
79 months, impacting different groundwater-dependent ecosystems. For instance, in *Quercus suber*
80 forests, which cover substantial portions of the Iberian Peninsula, groundwater accounts for 73.2%
81 of tree transpiration (Pinto et al., 2014). As climatic variability rises and water quality deteriorates,
82 the need for sustainable water management grows, especially in semi-dry climate regions like the
83 Iberian Peninsula (Grantham et al., 2008).

84 The southeastern corner of the Iberian Peninsula is expected to be one of the regions most affected
85 by climate change in Europe (Carvalho et al., 2021). Model predictions indicate that the
86 Mediterranean region, and particularly the Iberian Peninsula, will receive less precipitation while
87 temperature distributions are expected to shift toward higher mean (+2°C) and maximum (+4°C)
88 temperatures by the end of the century under the RCP8.5 scenario, along with increased drought
89 frequency and duration (Pereira et al., 2021). Moreover, future climate change is predicted to worsen
90 water stress and its severity in the Mediterranean area (Strada et al., 2023). Climate change in
91 Portugal is expected to significantly affect temperature and precipitation patterns, potentially
92 severely impacting crops such as vineyards (Wunderlich et al., 2023).

93 Machine learning (ML) is a powerful prediction tool for modelling groundwater level fluctuations
94 because of its ability to handle complex and nonlinear relationships between explanatory variables
95 and groundwater changes. Furthermore, it can be used to assess the uncertainty of model outputs
96 (Ahmadi et al., 2022; Seifi et al., 2020). In a study comparing ML and numerical models for simulating
97 groundwater dynamics, it was shown that multilayer perceptron (MLP), radial basis function (RBF),
98 and support vector machine (SVM) methods can perform as well or better than physically based
99 numerical models, such as MODFLOW (Chen et al., 2020). Also, artificial neural networks (ANN)
100 are effective tools for forecasting changes in groundwater levels (Guzman et al., 2017; Jeong and
101 Park, 2019; Müller et al., 2021; Wunsch et al., 2021; Zhang et al., 2020). Wunsch et al. (2021)
102 recently showed that 1D-convolutional neural networks (CNNs) outperform long short-term memory
103 (LSTM) models in terms of accuracy and calculation speed for simulating groundwater levels. CNNs
104 exhibited superior adaptability and consistency compared to nonlinear autoregressive models with
105 exogenous inputs (NARX) models. Because of their demonstrated precision, efficiency, reliability,
106 and versatility in handling diverse temporal patterns, CNNs were selected for the present study.
107 They excel at capturing both short-term fluctuations and long-term seasonal trends, making them
108 well-suited to model the direct effects of climatic factors on groundwater systems. Their ability to
109 efficiently process large datasets, identify complex hierarchical features, and adapt to various
110 temporal scales enhances their reliability for tasks involving spatially and temporally distributed data
111 across the Iberian Peninsula. Additionally, CNNs' computational efficiency, stemming from their
112 weight-sharing mechanism, minimizes overfitting risks while optimizing resource usage on modern
113 GPUs, further justifying their selection for this extensive regional-scale analysis.

114 Before investigating the indirect effects caused by regional and local human activities, which
115 certainly have a significant impact, it is crucial to first focus on the broader climate-driven influences.
116 Only the wells that appear to be unaffected by human activities will be considered as the projections
117 rely solely on meteorological variables. This approach is based on the expectation that future
118 changes in temperature and precipitation will be primary drivers of groundwater behaviour. For
119 example, on the Iberian Peninsula, significant fluctuations in precipitation and temperature have
120 already influenced groundwater recharge and availability (Diodato et al., 2024), highlighting the
121 importance of understanding climate-driven impacts for sustainable groundwater management. In
122 this study, we investigate the impact of climate change on groundwater levels, using temperature
123 and cumulative precipitation as explanatory variables, referred to hereafter as the direct impact of
124 climate change. The direct impact of climate change on groundwater is evident through various
125 mechanisms, such as increased temperatures leading to higher evaporation rates, reducing surface
126 water availability, and subsequently decreasing groundwater recharge (Cuthbert et al., 2019).
127 Climate change, characterized by rising temperatures, altered precipitation patterns, and increased
128 frequency of extreme weather events, has a profound impact on the global hydrological cycle.
129 Changes in precipitation patterns, with some areas experiencing prolonged droughts and others
130 intense rainfall, can disrupt the natural replenishment of aquifers (Neidhardt and Shao, 2023). This
131 disruption is particularly critical in regions like the Mediterranean, where future warming is expected
132 to exceed global rates, significantly affecting water availability (Cramer et al., 2018).

133 Below, we use the CNN deep learning methodology of Wunsch et al. (2022) to forecast groundwater
134 level changes. Our focus on understanding climate change impacts, so the models are driven by
135 gridded meteorological data. We apply it at various locations within the Iberian Peninsula using an
136 extensive database comprising 3829 wells with monitoring durations from 4 to 596 months. This
137 approach allows us to evaluate how groundwater levels may evolve under different representative
138 concentration pathway (RCP) scenarios. The specific objectives are to (i) evaluate the future direct
139 climate change impact (without considering the local human activities) on groundwater under the
140 RCP4.5 and 8.5 scenarios for three time periods: near- [2021-2040], mid- [2041-2060] and long-
141 term [2081-2100], (ii) explore the best explanatory variables including temperature and cumulative

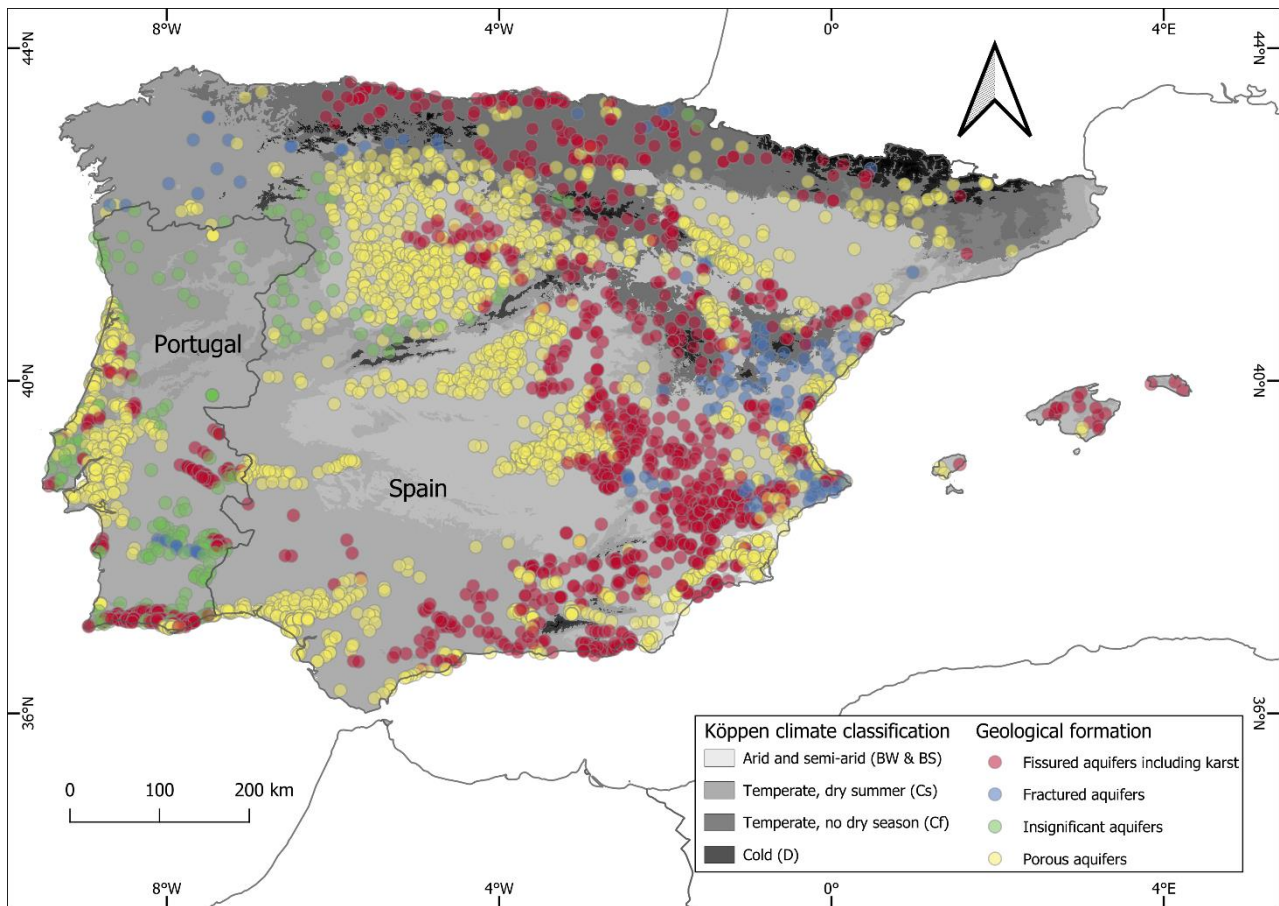
142 precipitation computed for different antecedent time lags (3, 6, 9, 12, 18, 24, and 36 months), and
143 (iii) identify the groundwater systems that are mainly controlled by climate forcing.

144 2. Materials and Methods

145 2.1. Data

146 We used a gridded dataset of daily precipitation and temperature over Iberia (Herrera et al., 2019,
147 2016) for historical climate data. Precipitation is considered a proxy for groundwater recharge, while
148 temperature is a proxy for evapotranspiration. Furthermore, temperature has a distinct yearly cycle,
149 which supplies the models with vital information on seasonality. This dataset (referred to as
150 Iberia01), developed using data from 3156 monitoring stations, consists of daily precipitation and
151 temperature data at a 0.1° regular resolution across the Iberian Peninsula from 1971 to 2015. The
152 meteorological influence at each well location was determined as the average precipitation and
153 temperature values from the nine surrounding grid cells of the Iberia01 dataset to reduce the
154 uncertainty. Other weighting schemes were assessed but were found to have little influence on the
155 results.

156 For historical groundwater data in Spain, we used data provided by the Ministry of Ecological
157 Transition and Demographic Challenge, which hosts a piezometric monitoring network
158 (<https://sig.mapama.gob.es/redes-seguimiento/>, last accessed 11 November 2024, data were
159 downloaded with a web scraping code in early 2020). In Portugal, groundwater data is managed in
160 a national hydrologic information system (<https://snirh.apambiente.pt/>, last accessed 11 November
161 2024). The data consist of records with variable durations, from 4 to 596 months and frequencies,
162 from monthly to bimonthly water table depth (WTD) measurements in both country databases as
163 meters below ground level (m b.g.l.). For consistency, data were downloaded in early 2020. The
164 analysed data comprised 940 wells in Portugal and 2889 wells in Spain, giving a total of 3829 wells.
165 **Figure 1** depicts the distribution of wells over the Iberian Peninsula along with their associated
166 geological formations, with the Köppen climate classification (Cui et al., 2021) shown in the
167 background.



168
169 **Figure 1.** Spatial distribution and geological formation of the 3829 groundwater level wells in the Iberian Peninsula.

170 2.2. Climate projections

171 For climate projections of daily precipitation and temperature, we utilised an ensemble of eight
172 combinations of general circulation models (GCMs) and regional climate models (RCMs) from the
173 Euro-Cordex initiative (Jacob et al., 2012), as delineated in **Table 1**. The spatial resolution of the
174 climate model data is 0.1° (EUR-11 grid), closely resembling that of the historical dataset (Iberia01).
175 These climate projections cover the period from 1950/1970 to 2100, comprising a historical
176 simulation until 2005 and the model predictions from 2006 to 2100.

177 Precipitation and temperature climate projections for each GCM/RCM combination were initially
178 interpolated onto the Iberia01 grid and then subjected to bias correction, using a distribution mapping
179 approach (D’Oria et al., 2017; Teutschbein and Seibert, 2012), based on the observed data from
180 the period 1976-2005 (further details are given in **Supplementary Material**, Bias correction). The
181 bias-corrected climate projections for the period 1976-2100 were obtained for RCP4.5 and 8.5.

182 **Table 1.** Ensemble of eight Euro-Cordex combinations of general circulation models (GCMs) and regional climate
183 models (RCMs) (M1-8) used for climate projections.

Abbreviation	GCM-RCM combinations
M1	CNRM_CERFACS_CNRM_CM5_CCLM4_8_1 7
M2	DMI_HIRHAM5_NorESM1-M
M3	ICHEC_EC_EARTH_HIRHAM5
M4	IPSL-INERIS_WRF381P_IPSL-CM5A-MR
M5	KNMI_CNRM-CM5
M6	MPI_M_MPI_ESM_LR_RCA4
M7	ICHEC-EC-EARTH_RACMO22E
M8	IPSL_IPSL_CM5A_MR_RCA4

2.3. Data selection and outlier removal

The raw WTD data consisted of a total of 3829 time series. Inspection of the raw data revealed that 21 wells lacked valid measurements and were eliminated from the database. For the purpose of training the deep learning models, the datasets were first screened based on two criteria: the total number of measurements in each time series and the percentage of missing measurements. Specifically, we only included datasets with less than 50% missing data and at least 120 valid measurements, which yielded 1205 wells for analysis. This technique ensured that the models were trained on the most extensive datasets available.

Outlier detection approaches are classified into two types: test discordance methods and labelling methods (Muthukrishnan and Poonkuzhali, 2017). Most outlier detection systems consider extreme values to be outliers. In this work, outliers were identified using the generalised extreme studentized deviate (ESD) test (Rosner, 1983) and excluded from model training. Among the most common outlier removal methodologies, the ESD method was used because it only needs as input an upper bound for the suspected number of outliers (Heckert et al., 2002). We chose the value of 10 for the maximum number of outliers for each time series, as suggested in the guidance for the PyAstronomy (Czesla et al., 2019) Python package.

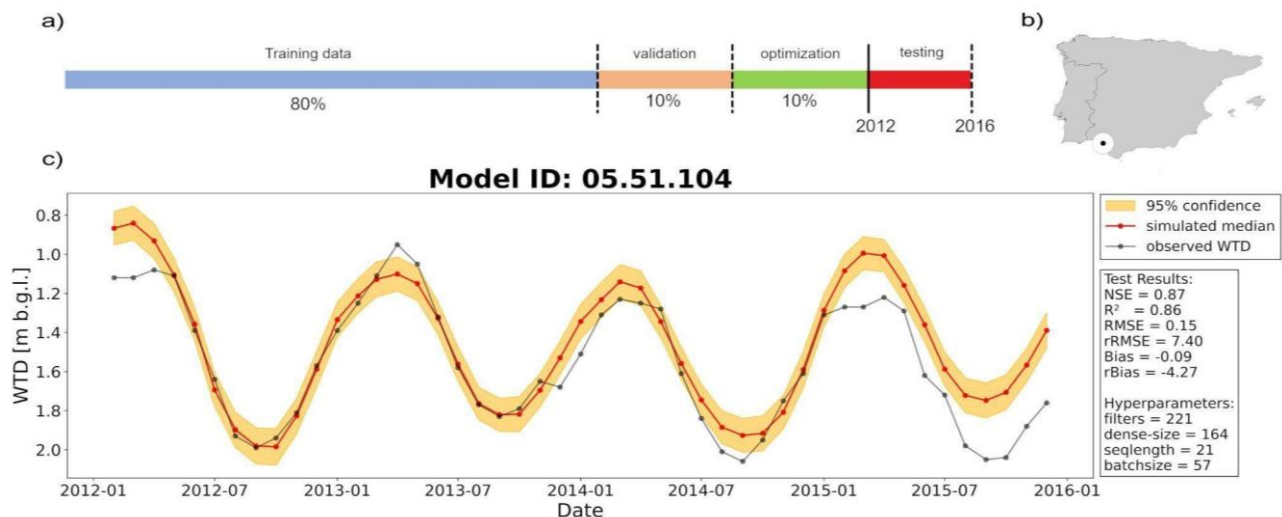
2.4. Model

We expanded on Wunsch et al. (2022), who only used temperature and precipitation as explanatory variables, by incorporating accumulated precipitation over various time periods (3, 6, 12, 18, 24, and 36 months) as additional variables. The convolutional neural networks (CNNs) used include layers designed to optimize model performance and prevent overfitting. We applied techniques like Monte-Carlo dropout, gradient clipping, and early stopping to improve model accuracy and robustness. Bayesian optimization was used to fine-tune the model's hyperparameters, and the entire process was built using Python and several key machine-learning libraries such as TensorFlow, Keras, and Scikit-Learn (further model description is given in **Supplementary Material**, Models setup).

2.5. Training and hyperparameter optimization

After finishing the pre-processing, we optimized key hyperparameters such as the number of filters, batch size, sequence length, and dense layer size. To do this, we used monthly WTD data from 1974 to 2015 and weather data, and split the time series into four sets: training, validation, optimization, and testing. The test period was always a four-year stretch, and adjustments were made when the data series ended early. The first 80% of the data before 2012 was used for training, and the rest was split evenly for validation and optimization during hyperparameter tuning. (**Figure 2a**) (Wunsch et al., 2022).

A maximum of 150 epochs was set for optimisation, stopping after 15 steps without improvement, provided at least 60 iterations had been performed. The data were scaled in the range $[-1, 1]$ and 10 different CNNs were built with randomly initialised weights. For each of the ten CNNs, we used Monte-Carlo dropout to estimate the model uncertainty from 100 realisations. The 95% confidence interval was then calculated using 1.96 times the standard deviation of the resultant distribution for each time step. To assess the model's accuracy, we computed various performance metrics, including the Nash-Sutcliffe efficiency (NSE), squared Pearson r (R^2), absolute and relative root mean squared error (RMSE, rRMSE), and absolute and relative Bias (Bias, rBias). The hyperparameters and test results are shown in **Figure 2c** for the well in the location indicated in **Figure 2b**.



227
 228 **Figure 2.** a) Time series splitting scheme for training (80%), validation (10%), optimization (10%), and testing (last four
 229 year) periods. b) Approximate location of the well in the region. c) Hyperparameters and model's performance using
 230 several statistical metrics for a random well (ID 05.51.104) during the test period [2012-2016].

231 2.6. Filtering models based on test results

232 CNNs were constructed for 1205 wells and filtered based on R² and NSE. Aimed at retaining those
 233 wells that could really be explained with temperature and precipitation, only those CNNs with NSE
 234 ≥ 0 and R² ≥ 0.5 were retained, resulting in a final selection of 170 wells. **Figure S1**
 235 (**Supplementary Material**) presents a scatter plot showing the NSE and R² values for all locations,
 236 highlighting the selected ones.

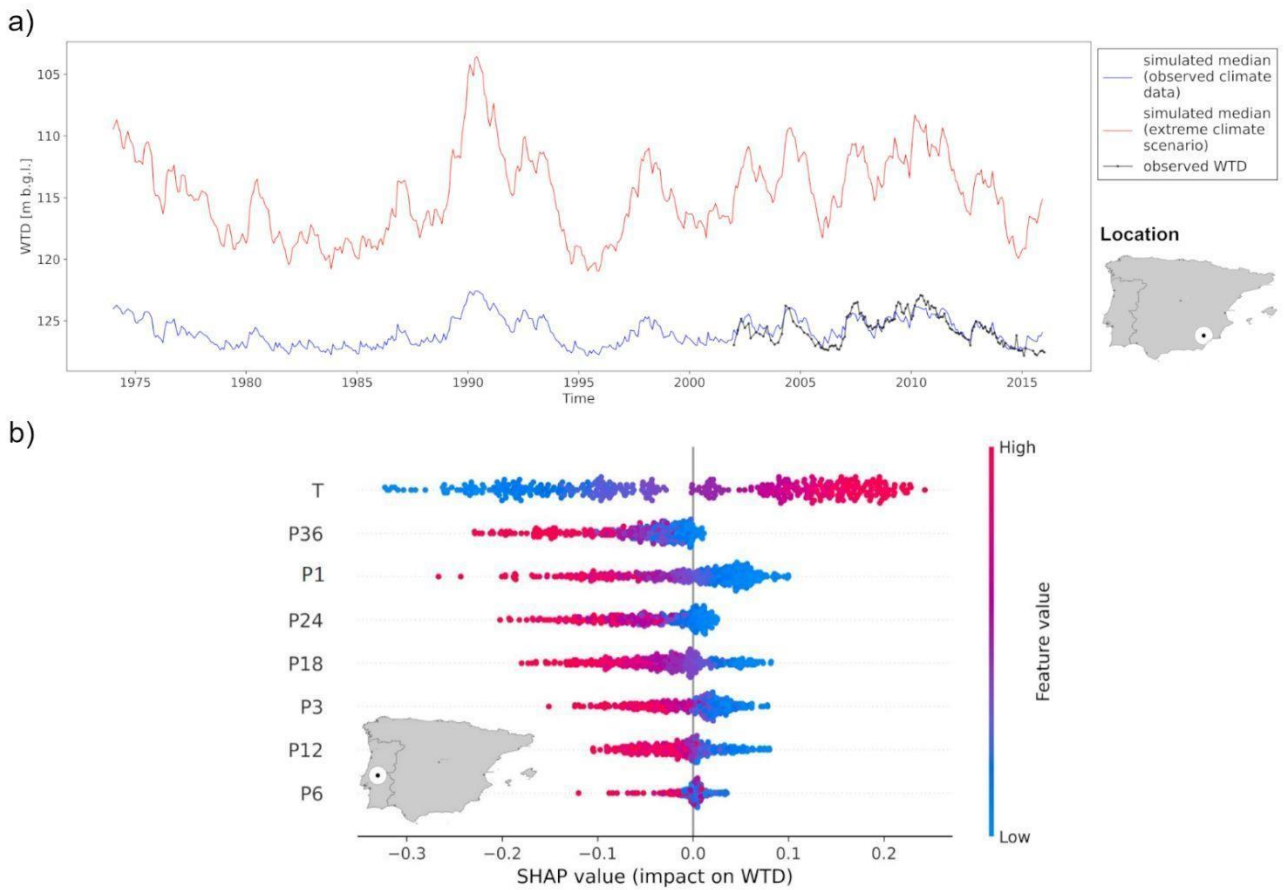
237 2.7. Model evaluation

238 A plausibility test of the 170 CNN models was performed by analysing their behaviour for explanatory
 239 variable values outside the range of the training data. We retrained all models with hyperparameters
 240 from Section 2.6 and data until 2016. Data time series were divided into two parts: 80% for training
 241 and 20% for early stopping.

242 The retrained models were used to simulate well evolution assuming four times the precipitation and
 243 a uniform 5°C temperature rise with respect to the historical data in the training set (Duan et al.,
 244 2020) (**Figure 3a**). As expected, higher precipitation and temperatures produce larger oscillations
 245 in WTD. SHapley Additive exPlanations (SHAP) were used to identify how each explanatory variable
 246 contributes to the model's prediction for a specific instance. **Figure 3b** shows a SHAP summary plot
 247 for one of the wells (typical results shown). Each dot corresponds to one of the times over which the
 248 prediction is performed. A positive SHAP value indicates that a given feature drives the prediction
 249 above its average, and a negative one, the contrary. The larger the SHAP magnitude, the more
 250 important the feature is to explain the model prediction.

251 Thus, the results in **Figure 3b** show that elevated temperatures, which tend to induce larger
 252 evapotranspiration, result in a rise in WTD (i.e., depletion of groundwater levels), whereas high
 253 precipitation, which produces more recharge, drives WTD to decrease (groundwater recharge). The
 254 SHAP values are consistent with known aquifer responses to changes in meteorological forcing.

255 In this phase, we assessed all 170 models using results from extreme conditions to ensure the
 256 stability of the models and analysed SHAP summary plots to confirm that the direction of the
 257 explanatory variables aligned with physical understanding of the groundwater system. Additionally,
 258 we evaluated the models based on rBias and rRMSE, ensuring that both metrics fell within a $\pm 25\%$
 259 range. Models that did not meet these criteria were eliminated. Following this comprehensive
 260 evaluation, 92 wells were selected for further analysis.



261
262
263
264
265

Figure 3. a) Plausibility Check under extreme conditions for a typical well (ID 07.26.001). Model output under an artificial extreme climate scenario in the past (1974 - 2015) along with the location of the well. **b)** SHAP summary plot for well (ID 331.89) and its approximate location. [P1, P3, ..., P36] are accumulated precipitation values for [1, 3, ..., 36] months and T is the average monthly temperature.

266

2.8. Model selection

267

268

269

270

271

272

273

274

275

276

To analyse the impact of climate change on groundwater in the Iberian Peninsula, we focus on the 92 best-performing CNN models. These models are those for which the CNNs were able to predict groundwater fluctuations in response to temperature and precipitation data; this behaviour could be interpreted as that the 92 retained CNN wells were mainly controlled by climate variables. The **Supplementary Material (Figures S2-S93)** contains the results of the hyperparameter optimization test, extreme conditions, and SHAP summary plots for all 92 wells.

At the next step, we forecasted the WTD for each well using the eight Euro-Cordex models (M1-M8) in **Table 1** for two distinct climate change scenarios—RCP4.5 as the best-case scenario and RCP8.5 as the worst-case. This yields a total of 16 projection outcomes for each well (eight for each RCP scenario).

277

2.9. Evaluation of results

278

279

280

281

282

283

Following the projections for the 92 retained models, we examined changes in WTD along with a detailed analysis of their depths and historical trends. The changes were calculated using the following process: For each climate scenario, the annual median values from the eight models were first calculated. The average of these median values for both the 20-year reference period and the 20-year future projection period were computed, and the difference between these two averages represents the reported change. The equation used was:

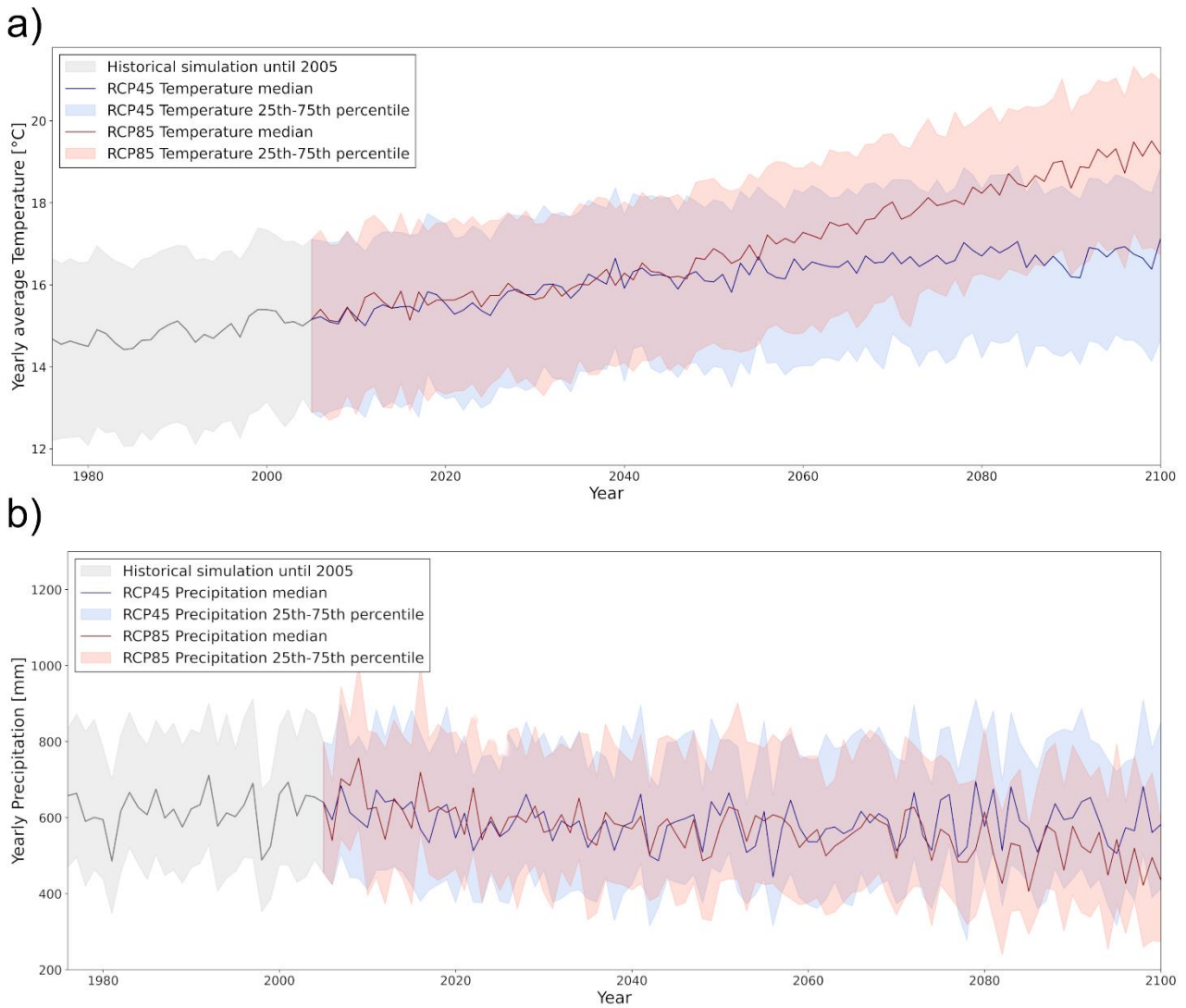
284

$$\Delta WTD = \frac{1}{20} \sum_{y=1}^{20} \left(\text{med}(WTD_{y,M1}, \dots, WTD_{y,M8}) \right)_{fut} - \frac{1}{20} \sum_{y=1}^{20} \left(\text{med}(WTD_{y,M1}, \dots, WTD_{y,M8}) \right)_{ref}$$

285
286 where ΔWTD is the change displayed in the figure, $med(WTD_{y,M1}, \dots, WTD_{y,M8})$ denotes the median
287 WTD from the eight different models (M1-M8) for year y , and the summation refers to the averaging
288 over the 20-year time period considered (*ref*: refers to the reference period [1986-2005], while *fut*:
289 refers to the future periods [2021-2040], [2041-2060] or [2081-2100] which corresponds to short-,
290 mid- and long-term, respectively).
291 Additionally, we examined the significance of aquifer depth on the climate change impact. We used
292 the maximum historical water table depth for each well as an indicator to classify them considering
293 a depth threshold of 50 m for shallow aquifers,
294 As previously stated, our models focus solely on climatic data, specifically the direct impact of
295 climate change on groundwater levels, with precipitation and temperature being the primary direct
296 drivers (Taylor et al., 2012; Wu et al., 2020). We used the Mann-Kendall test considering 5%
297 significance level ($P < 0.05$) to evaluate trends in the historical groundwater level data for the same
298 period as in model training. We performed the modified Mann-Kendall test with the Trend-Free Pre-
299 Whitening method proposed by Yue and Wang (2002) to mitigate the effects of serial correlation.

300 3. Results

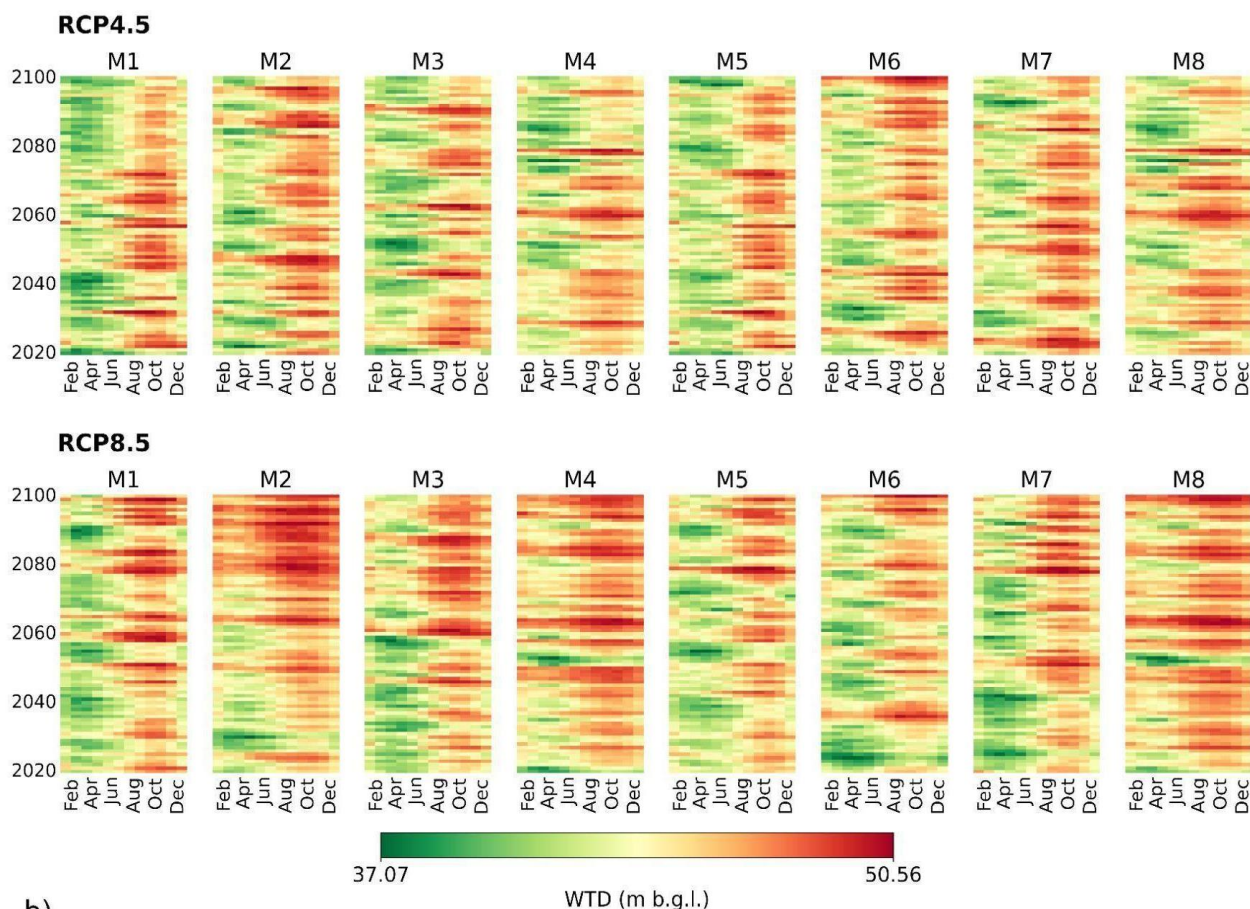
301 Analysis of yearly average temperature and precipitation data for the reference period [1986-2005]
302 and the long-term period [2081-2100] reveals notable changes under both the RCP4.5 and RCP8.5
303 scenarios. The yearly average temperature under RCP4.5 is projected to increase from 15.0°C
304 during the reference period to 16.7°C in the long-term period, a rise of 1.7°C. Under the more
305 extreme RCP8.5 scenario, the yearly average temperature is projected to increase by 3.9°C from
306 15.0°C to 18.9°C (**Figure 4a**).
307 The yearly average precipitation is projected to decline for both scenarios. Under RCP4.5, the
308 annual precipitation decreases from 624 mm in the reference period to 592 mm in the long-term
309 period, with an absolute decrease of 32.8 mm, equivalent to a 5.2% reduction. The RCP8.5 scenario
310 exhibits a more pronounced decline, with the annual precipitation decreasing from 624 mm to 498
311 mm, representing an absolute decrease of 126 mm, or 20.2% (**Figure 4b**).



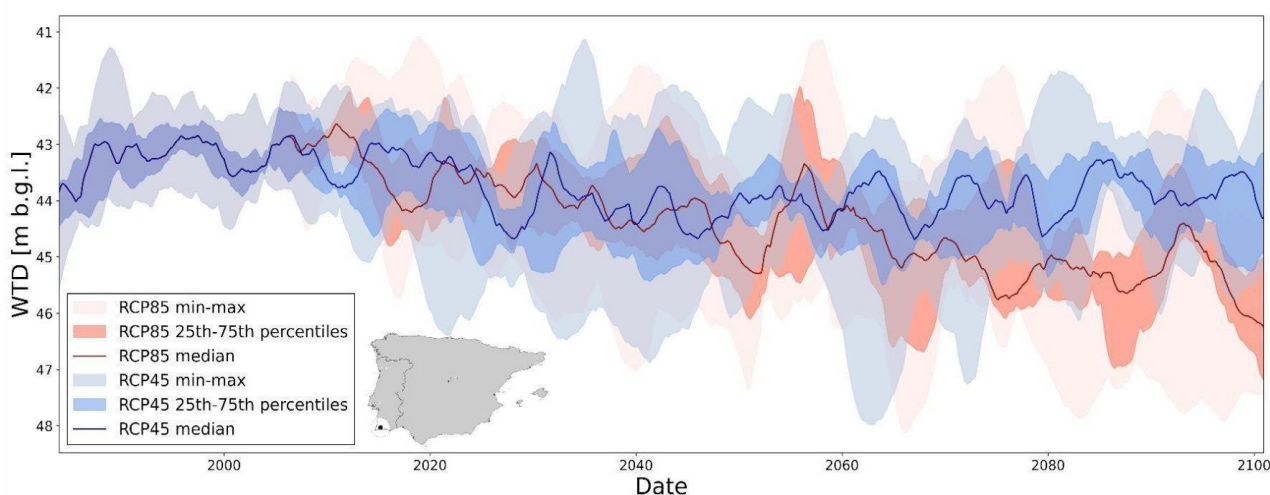
312
 313 **Figure 4.** a) Median line and uncertainty band of temperature projection data of 92 well locations and eight ensemble
 314 climate projection models under the RCP 4.5 and 8.5 scenarios. b) The same results for annual precipitation.

315 **Figure 5a** presents a heatmap of the projected WTD for a typical well (ID: 594.34) from 2020 to
 316 2100. This figure compares predictions from eight different climate models under two RCP
 317 scenarios. The top row corresponds to the RCP4.5 scenario, and the various model predictions
 318 while the lower row corresponds to the RCP8.5 scenario. Under the RCP4.5 it is observed that most
 319 models indicate a relatively stable condition by not showing intense red tones in the long-term period
 320 [2080-2100] in water levels, except model M2 that shows a more extreme drop in groundwater levels
 321 towards the end of the century. The difference in model simulations (M1-M8) underscores the
 322 uncertainty level associated with climate change projection.

a)



b)



323
324
325
326
327
328

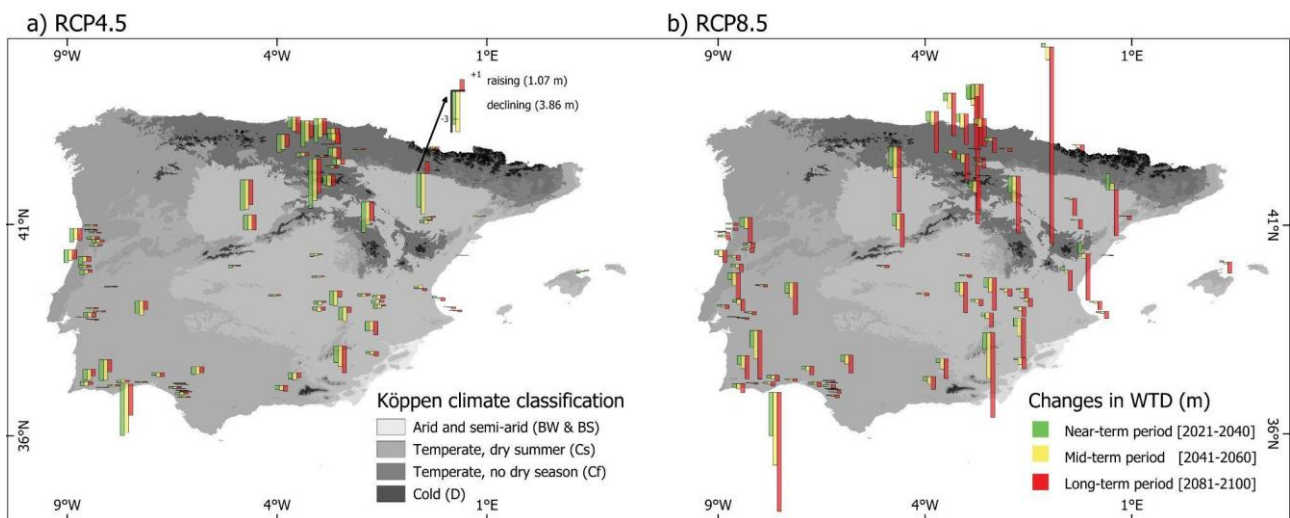
Figure 5. a) Heatmaps of water table depth (WTD) for a typical well (ID 594.34) under different climate scenarios (see Table 1). The top row represents RCP4.5, and the second row represents RCP8.5. The heatmaps cover the simulation period from 2020 to 2100 for each climate model projection within the respective scenario. **b)** Projections of WTD until 2100, showing the 5-y moving average, 25th-75th percentile range, and min-max range of the median values from eight models for both RCP4.5 and RCP8.5. The approximate location of the well is indicated in the map next to the legend.

329
330
331
332
333
334

Unsurprisingly, under RCP8.5 (second row in **Figure 5a**), the influence of climate change on groundwater levels is more pronounced than for RCP4.5. The deviation between the RCP4.5 and RCP8.5 predictions begin in the mid-term period [2041-2060] and intensifies as the long-term period [2081-2100] approaches. It is evident that the M2 model shows the greatest decline in groundwater levels compared to other models, which is also observed for RCP4.5 scenario in the long run. As might be expected, all models exhibit the most significant impact during the long-term period [2081-

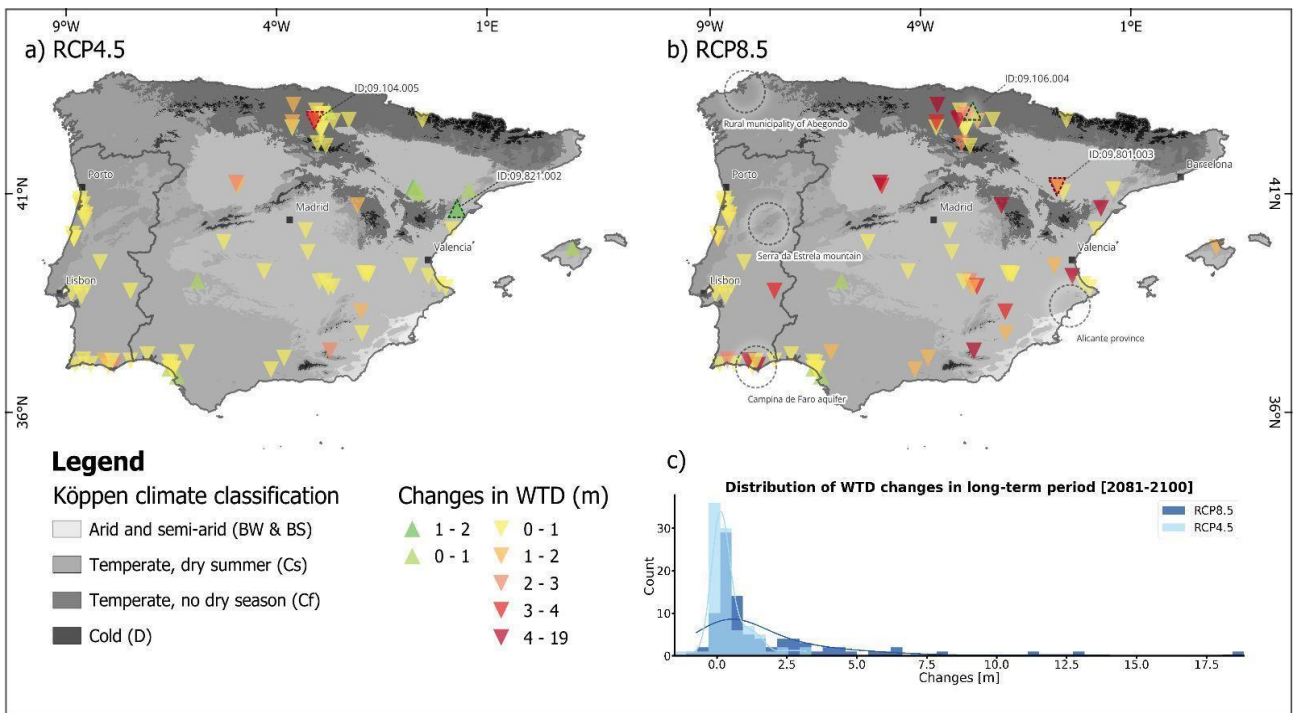
335 2100]. To assess the uncertainty associated with future scenarios and model predictions, **Figure 5b**
 336 presents the median, 25th-75th percentile interval, and min-max range obtained from the ensemble
 337 of climate models for both scenarios. To smooth the results, we computed all these statistics based
 338 on a 5-y moving average of the predictions. **Figure 5b** indicates that, despite variations, the medians
 339 of the two scenarios are comparable and relatively stable between 2006 and 2060, after which they
 340 begin to diverge from each other with the largest differences toward the end of the century. In the
 341 **Supplementary Material (Figures S94–S185)**, heatmaps and predictions for all 92 wells are
 342 provided.

343 **Figure 6** illustrates the magnitude of the predicted changes during each of the three analysed
 344 periods under the two RCP scenarios. The results show that under the RCP8.5 scenario, changes
 345 are more pronounced than under RCP4.5. For the RCP8.5 scenario, the magnitude of the WTD
 346 changes tends to escalate as the century progresses, with the most significant changes occurring
 347 in the long-term period. On the other hand, for the RCP4.5 scenario, there is no clear trend, and for
 348 some wells, the long-term changes are even smaller than the mid- and short-term ones.
 349 Each well in **Figure 6** is represented by a set of three bars, each indicating the absolute changes in
 350 WTD from the reference period [1986-2005] to the respective future time periods. The bars
 351 correspond to the short-term [2021-2040], mid-term [2041-2060], and long-term [2081-2100]
 352 periods.



353 **Figure 6.** Bar charts of WTD changes under RCP4.5 (a) and RCP8.5 (b) during the near-term [2021-2040], mid-term
 354 [2041-2060] and long-term [2081-2100] periods compared to the reference period [1986-2005].
 355

356 Results in **Figure 7a, b** show changes only in the long-term period under both climate scenarios.
 357 Under the RCP4.5 scenario, 10.9% of the wells show a rise between 0 and 2 m (the highest rise is
 358 1.5 m for well 09.821.002, see the location in the figure), while the rest of the wells display a decline.
 359 This decline is between 0 and 1 m for 73.9% of the wells, 15.2% of the wells show drops > 1 m with
 360 the highest predicted decline being 3.2 m for well 09.104.005. In comparison, under the RCP8.5
 361 scenario, a smaller fraction of wells (5.0%) shows a rise (the highest rise is 0.7 m for well
 362 09.106.004), while the rest display a decline. This decline is between 0 and 1 m for 55.0% of the
 363 wells, 40% shows drop > 1 m with the highest predicted decline being 18.8 m for well 09.801.003.
 364 The histograms of the changes are shown in **Figure 7c** for both scenarios. The result clearly
 365 illustrates that the range of WTD changes under RCP4.5 is narrower than that for RCP8.5 and that
 366 the median for RCP4.5 is smaller than for RCP8.5, resulting in a more skewed distribution for
 367 RCP8.5 than for RCP4.5.
 368

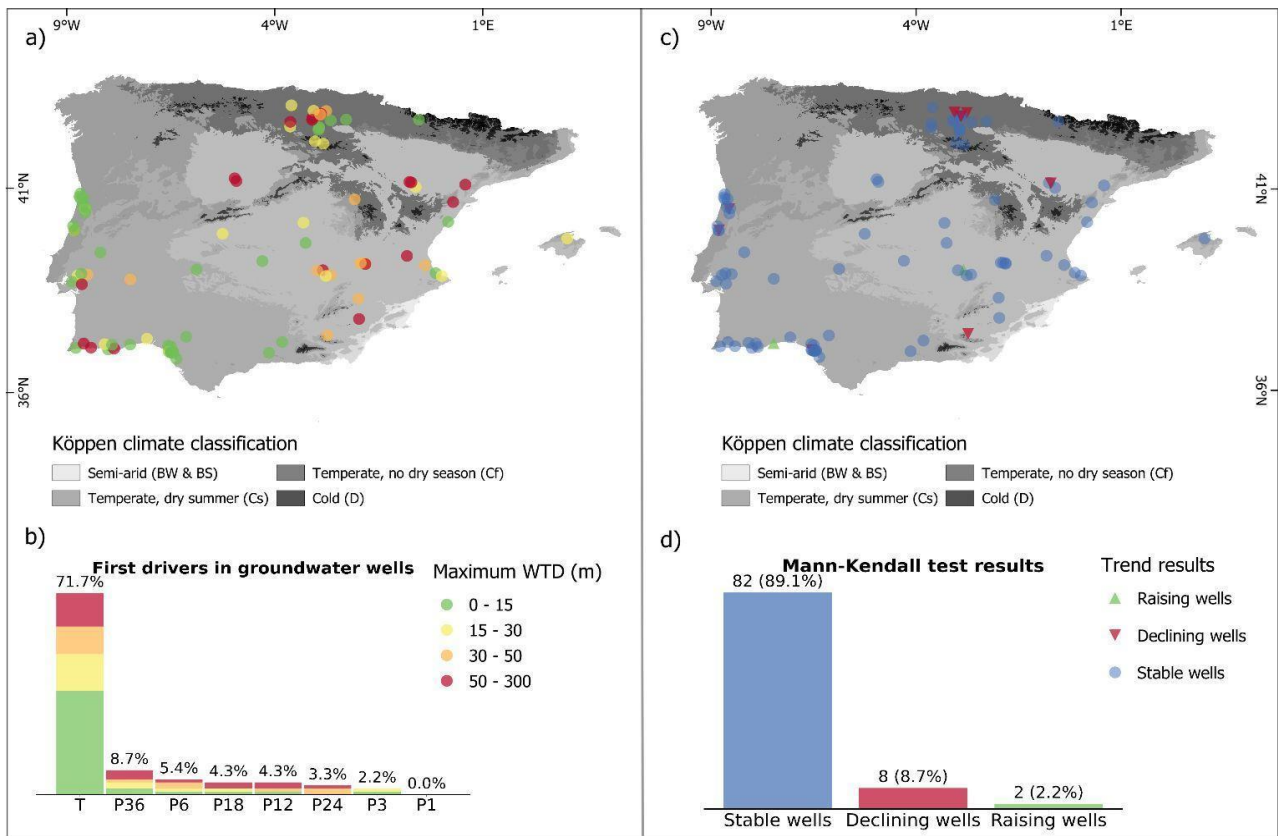


369
370
371

Figure 7. WTD changes in under RCP4.5 (a) and 8.5 (b) during the long-term period [2081-2100] compared to the reference period [1986-2005]. c) Comparison between RCP8.5 and RCP4.5 histogram of changes in both scenarios.

372 As described in the methodology section, eight explanatory variables: temperature and cumulative
373 precipitation over periods ranging from 1 to 36 months. Utilising SHAP values with each CNN model,
374 we identified the dominant driver of groundwater level changes. In more than 70% of the models,
375 temperature is the most influential driver, implying that evaporation has a greater impact on
376 groundwater levels than precipitation.

377 The significance of aquifer depth was further examined in relation to climate change impacts. Among
378 the 92 studied wells, 20 have depths greater than 50 m, with 7 of these exceeding 100 m. The
379 average depth across all wells is 36 m, and the deepest water table reaches 290 m, based on
380 historical records. This depth distribution may modulate how temperature and precipitation influence
381 groundwater levels across varying depths (Figure 8a, b). Notably, almost 90% of the wells exhibited
382 no trend during the training period considered (Figure 8c, d).



383
384
385
386
387

Figure 8. a) Classification of 92 selected wells based on the maximum water table depth (WTD) during the historical period, with b) the stacked bar chart representing the dominant explanatory variable (temperature) based on SHAP value results. c) Modified Mann-Kendall test results based on the yearly historical data used for the training period. d) Bar chart showing the trend analysis results.

388

4. Discussion

389
390
391
392
393

Despite historically stable or increasing groundwater levels over recent decades (Chávez García Silva et al., 2024; Scanlon et al., 2023), projections from this study under the RCP4.5 and RCP8.5 climate scenarios suggest significant potential declines. These scenarios underscore the increased vulnerability of shallow groundwater to the impacts of climate change in the Iberian Peninsula (Barredo et al., 2018).

394

4.1. Importance of small changes

395
396
397
398
399
400
401
402
403
404
405
406
407
408
409

Although a groundwater decline of 1 m might not seem significant in a period of around 90 y, it is important to note that the models only consider the direct impact of climate change on groundwater levels. Climate change can directly impact groundwater levels through changes in precipitation patterns and intensity (Barredo et al., 2018), and a decrease in precipitation can lead to reduced groundwater recharge, resulting in lower groundwater levels. Similarly, lower levels are likely for temperature increases due to greater evapotranspiration and reduced soil moisture (Hunkeler et al., 2022; Odwori, 2022). Climate change can also indirectly affect groundwater levels through changes in land use and domestic as well as crop/vegetation water demand. As the climate changes, agricultural practices and water usage patterns may shift, potentially resulting in increased groundwater extraction for irrigation. This overexploitation of groundwater resources can lead to significant additional declines in groundwater levels (Davamani et al., 2024; Khoso et al., 2024). Changes in groundwater levels can greatly affect the ecological services provided by groundwater and its sustainable management. This is particularly true for ecosystems that rely on groundwater during low-flow conditions when it becomes scarce. Changes in groundwater depth can impact soil properties, which can subsequently alter surface vegetation characteristics (Dong et al., 2023;

410 Scanlon et al., 2023). In the Iberian Peninsula, groundwater depletion can significantly affect soil
411 moisture dynamics and evapotranspiration fluxes, particularly in shallow water table regions where
412 groundwater is hydraulically connected to the upper soil through upward capillary fluxes (Llamas et
413 al., 2015). Although we consider only the direct impact of climate change on groundwater levels, it
414 is important to recall that foreseen circumstances such as lengthy droughts (Gómez-Martínez et al.,
415 2021) would potentially lead to over-pumping of groundwater to cope with water stress resulting in
416 further drop in water levels (Taylor et al., 2012). In summary, the changes we forecast are the
417 minimum ones, and they will be worsened by other actions induced by climate change.

418 4.2. Similar previous studies

419 Several studies have investigated the impact of climate change on groundwater levels within specific
420 aquifers in the Iberian Peninsula, whereas our study examines the entire region. For instance,
421 Samper et al. (2022) used a semi-distributed water balance model to assess changes in
422 groundwater recharge in the municipality of Abegondo in Galicia, Spain (annotated in **Figure 7b**),
423 projecting a reduction in recharge by 6-10% by the end of the century. Similarly, Costa et al. (2021)
424 evaluated the Campina de Faro aquifer in southern Portugal using a 3D groundwater flow and nitrate
425 transport model (FEFLOW), finding that climate change, along with agricultural practices, could lead
426 to groundwater depletion and potential salinization. In another study, Moutahir et al. (2017) utilized
427 the VISUAL-BALAN model in a Mediterranean region of southeastern Spain, forecasting decreases
428 in groundwater recharge and streamflow, particularly under RCP8.5. Furthermore, Pisani et al.
429 (2019) examined the Serra da Estrela region in central Portugal, predicting reductions in aquifer
430 recharge and streamflow using water balance models.

431 These studies, although conducted on an aquifer scale, generally align with our findings, confirming
432 that climate change significantly influences groundwater levels. However, these studies employed
433 process-based models that require the incorporation of a large amount of data including:
434 groundwater recharge, soil properties such as hydraulic conductivity, land use, agricultural
435 practices, and abstraction rates, alongside climate variables like precipitation and temperature. The
436 present study, in contrast, employs deep learning (CNN models) on a regional scale, using
437 temperature and accumulated precipitation as the only explanatory variables to isolate the direct
438 impact of climate change on groundwater levels. While aquifer-scale studies provide valuable
439 localized insights and consider both climatic and anthropogenic factors, our approach offers a
440 simpler data-driven approach that captures the spatial variability and climate-driven trends across
441 the entire Iberian Peninsula.

442 Among the explanatory variables considered, temperature, which strongly influences
443 evapotranspiration, has a greater impact than precipitation, confirming previous findings (Wunsch
444 et al., 2022). Furthermore, we used cumulative precipitation data as explanatory variables to capture
445 the time lag between precipitation events and groundwater response. While temperature was the
446 dominant factor influencing groundwater levels, P36 (cumulative precipitation over 36 months)
447 emerged as the main driver for 8.7% of the wells. This was followed by P6, P18, P12, P24, and P3,
448 as shown in **Figures 8a, b**. As expected, P1 (precipitation over one month) was not identified as the
449 main driver for any of the wells, indicating that long-term cumulative precipitation has a stronger
450 influence on groundwater levels than short-term precipitation.

451 These results agree with numerous studies that emphasize the importance of accumulated long-
452 term precipitation towards changes in groundwater levels. For instance, Jan et al. (2007) showed
453 that groundwater level variations follow short-run and long-run cumulative rainfall, as evidenced in
454 their work on the Donher well station in Central Taiwan. They found that the cumulated rainfall over
455 10 d was more influential in groundwater levels than shorter periods. They attributed this to the
456 typically delayed response of groundwater to rainfall, wherein past rainfall contributes much to the
457 current water table conditions. By using an exponential-decay weighting technique to determine

458 effective cumulative rainfall, they showed that older precipitation events continue to affect
459 groundwater levels, although their influence becomes weaker over time (Jan et al., 2007).
460 Further, the Wisconsin study (Smail et al., 2019) trend of CDM60 (cumulative deviation from 5-y
461 moving mean precipitation) indicated that groundwater levels are more correlated with long-term
462 than short-term precipitation oscillations. This further reinforces the concept that groundwater
463 systems take successive periods of surplus precipitation to alter their levels drastically. Thus, it is
464 expected that P1 lacks influence, while more seasonable measures like P36 are responsible for
465 groundwater responses to significant precipitation.
466 The deep learning algorithm identifies the relationship between input parameters, precipitation and
467 temperature, and the output parameter, groundwater level. The 92 wells are those where
468 groundwater levels can be described well using only these input parameters, thereby implying that
469 the influence of external or anthropogenic pressures is minimal. As evidenced by the trend analysis,
470 90% of the wells exhibited no trend during the training period, indicating that they are naturally in a
471 stable condition and not under heavy stress. Consequently, we can conclude that these wells are
472 not subject to significant anthropogenic or any other pressure (**Figure 8c, d**).
473 A recent study examining groundwater level trends Chávez García Silva et al. (2024) covered the
474 period from 1960 to 2020 across Spain, Portugal, France, and Italy, and similarly found that 68% of
475 wells remained stable over this time, with an additional 20% showing rising levels. These findings
476 underscore the resilience of many groundwater systems to external influences during the historical
477 period, especially in temperate regions. However, the situation for groundwater wells in the future is
478 projected to change significantly. While both studies highlight a period of relative stability in the past
479 and near future, our future projections based on climate models and deep learning algorithms
480 indicate that future conditions will likely shift towards declining groundwater levels. The anticipated
481 reduction in precipitation and increased temperatures, which exacerbate evapotranspiration and soil
482 moisture deficits, suggest that wells that are currently stable could experience depletion in the
483 coming decades due to climate change.
484 Of the 92 wells, 72 have a depth of 50 m or less, indicating that approximately 78% are in shallow
485 aquifers (**Figure 8b**). This distribution suggests that shallow aquifers are more influenced by climate
486 variability and change, responding quickly to surface climatic conditions due to shorter lag times. A
487 recent study by Gumuła-Kawęcka et al. (2023) supports this, demonstrating that shallow aquifers in
488 northern Poland have shown significant responses to climate change over the past 70 y. In contrast,
489 deeper aquifers exhibit greater resilience to climate impacts and serve as more stable, long-term
490 freshwater storage due to their reduced sensitivity to surface conditions. This finding is consistent
491 with Zhou et al. (2022), who studied the hydrochemical background levels and threshold values of
492 phreatic groundwater in the Greater Xi'an Region, China, underscoring the importance of
493 understanding aquifer characteristics for effective water quality management.

494 4.3. Challenges and perspectives

495 The Iberian Peninsula was chosen for its relatively dense and accessible groundwater data
496 compared to other regions, yet only a few wells were retained for further analysis. Dropped wells
497 were excluded primarily due to inconsistencies in regional monitoring strategies, including variability
498 in frequency, duration, and completeness of the time series. Many historical groundwater time series
499 suffer from short durations, irregular frequencies, and a lack of uniformity, all of which impact model
500 training quality. Additionally, wells influenced by human activities, such as irrigation and domestic
501 use, are unsuitable for our approach, which considers climate variables exclusively as controlling
502 factors of groundwater changes. Comprehensive information of the effects of anthropogenic activities
503 on groundwater levels remains challenging in the region due to fragmented monitoring of key drivers
504 (Deines et al., 2019; Leduc et al., 2017). Furthermore, including more climate forcing parameters like
505 soil moisture, surface net solar radiation and finding a suitable proxy parameter to capture the

506 anthropogenic pressures on groundwater levels (such as groundwater abstraction) would also be
507 highly beneficial. Numerous studies have utilized Earth Observation data to assess anthropogenic
508 pressures on groundwater levels. Barron et al. (2014) used Sentinel-1 SAR data to identify
509 groundwater-dependent vegetation. Similarly, numerous studies combined remote sensing data with
510 hydrological and hydrogeological modelling results to capture human-induced groundwater depletion
511 across scales (Abdelkareem et al., 2023; Döll et al., 2014; Guermazi et al., 2019). In the case of the
512 Iberian Peninsula, similar methodologies have been applied, including the use of multispectral
513 satellite imagery to map irrigated crops in Spain (Garrido-Rubio et al., 2018) as well as integration of
514 global groundwater models with in situ observations for assessment of the status of groundwater
515 resources and the impact of human activities on groundwater levels (Ben-Salem et al., 2023).
516 Future research could explore the use of multi-well training approaches alongside training individual
517 models for each well. Multi-well training has gained popularity in recent years due to its potential
518 advantages, such as predicting groundwater levels in areas with insufficient historical in situ data.
519 However, these approaches do not consistently provide better accuracy compared to single-well
520 training methods. As an example, Chidepudi et al. (2023) and Heudorfer et al. (2024) demonstrated
521 that while deep learning models trained on multiple wells can effectively capture broader hydrological
522 patterns, they do not always outperform models trained on individual wells in terms of predictive
523 accuracy. By utilizing data from all available piezometric stations, multi-well models can identify
524 relationships or events that might occur at a target location, even if not previously observed there.

525 5. Conclusions

526 In a future characterised by rising temperatures and decreasing precipitation (RCP8.5), groundwater
527 resources will face significant stress. However, by limiting greenhouse gas emissions (RCP4.5),
528 long term impacts of climate change on the depletion of groundwater levels are limited. Groundwater
529 level changes under RCP8.5 intensify over time, with more severe impacts observed over the long
530 term [2080–2100], while under RCP4.5, groundwater levels remain relatively stable, with occasional
531 decreases.

532 Using deep learning, we developed CNN models with high computational speed irrespective of the
533 availability of local geological or geophysical information. Only temperature and cumulated
534 precipitation (the latter to account for the time lag between the actual precipitation event and the
535 aquifer response), were used to identify the direct impact of climate change on groundwater levels.
536 While the indirect impact related to human activities were not considered in our study, they could
537 have even more severe consequences for groundwater. To address both climate and anthropogenic
538 impacts and safeguard groundwater resources, effective management strategies must be
539 implemented to optimize water consumption and enhance groundwater recharge. These include
540 managed aquifer recharge techniques, adoption of water-saving irrigation practices, and
541 prioritization of nature-based solutions. While groundwater aquifers will continue to be a vital and
542 resilient resource, their long-term sustainability will depend on prompt and effective mitigation
543 actions.
544

545 CRediT authorship contribution statement

546 **Amir Rouhani:** Conceptualization, Data curation, Formal analysis, Methodology, Software,
547 Visualization, Writing – original draft, Writing – review & editing. **Nahed Ben-Salem:** Data curation,
548 Investigation, Writing – review & editing. **Marco D'Oria:** Data curation, Methodology, Writing –
549 review & editing. **Rafael Chávez García Silva:** Data curation, Writing – review & editing. **Alberto**
550 **Viglione:** Writing – review & editing. **Nadim K. Copty:** Writing – review & editing. **Michael Rode:**
551 Writing – review & editing. **David Andrew Barry:** Methodology, Writing – review & editing. **J. Jaime**

552 **Gómez-Hernández:** Methodology, Writing – review & editing. **Seifeddine Jomaa:**
553 Conceptualization, Funding acquisition, Methodology, Supervision, Writing – review & editing.
554

555 Declaration of competing interest

556 The authors declare no competing financial interests or personal relationships that could influence
557 the work reported in this paper.
558

559 Data availability

560 All the data utilised in this study are freely accessible online.
561

562 Acknowledgments

563 This work was supported by the OurMED PRIMA Program project funded by the European Union's
564 Horizon 2020 Research and Innovation programme under grant agreement No. 2222.
565

566 References

- 567 Abdelkareem, M., Abdalla, F., Fahad Alshehri, Pande, C.B., 2023. Mapping Groundwater
568 Prospective Zones Using Remote Sensing and Geographical Information System Techniques
569 in Wadi Fatima, Western Saudi Arabia. *Sustainability* 15, 15629–15629.
570 <https://doi.org/10.3390/su152115629>
571
- 572 Adams, K.H., Reager, J.T., Rosen, P., Wiese, D.N., Farr, T.G., Rao, S., Haines, B.J., Argus, D.F.,
573 Liu, Z., Smith, R., Famiglietti, J.S., Rodell, M., 2022. Remote Sensing of Groundwater: Current
574 Capabilities and Future Directions. *Water Resour Res* 58, e2022WR032219.
575 <https://doi.org/10.1029/2022WR032219>
- 576 Ahmadi, A., Olyaei, M., Heydari, Z., Emami, M., Zeynolabedin, A., Ghomlaghi, A., Daccache, A.,
577 Fogg, G.E., Sadegh, M., 2022. Groundwater Level Modeling with Machine Learning: A
578 Systematic Review and Meta-Analysis. *Water (Switzerland)* 14, 949.
579 <https://doi.org/10.3390/W14060949>
- 580 Alley, W.M., Healy, R.W., LaBaugh, J.W., Reilly, T.E., 2002. Flow and Storage in Groundwater
581 Systems. *Science* 296, 1985–1990. <https://doi.org/10.1126/science.1067123>
582
- 583 Barredo, J.I., Mauri, A., Caudullo, G., Alessandro Dosio, 2019. Assessing Shifts of Mediterranean
584 and Arid Climates Under RCP4.5 and RCP8.5 Climate Projections in Europe. *Pageoph topical*
585 *volumes* 235–251. https://doi.org/10.1007/978-3-030-11958-4_14
586
- 587 Barron, O. V., Emelyanova, I., Van Niel, T.G., Pollock, D., Hodgson, G., 2014. Mapping
588 groundwater-dependent ecosystems using remote sensing measures of vegetation and
589 moisture dynamics. *Hydrol Process* 28, 372–385. <https://doi.org/10.1002/HYP.9609>
- 590 Ben-Salem, N., Reinecke, R., Coptly, N.K., Jaime Gómez-Hernández, J., Varouchakis, E.A.,
591 Karatzas, G.P., Rode, M., Jomaa, S., 2023. Mapping steady-state groundwater levels in the
592 Mediterranean region: The Iberian Peninsula as a benchmark. *J Hydrol* 626, 130207.
593 <https://doi.org/10.1016/J.JHYDROL.2023.130207>
- 594 Burchi, S., Mechlem, K., n.d. FAO LEGISLATIVE STUDY 86 UNITED NATIONS EDUCATIONAL,
595 SCIENTIFIC AND CULTURAL ORGANIZATION FOOD AND AGRICULTURE
596 ORGANIZATION OF THE UNITED NATIONS Rome, 2005 Groundwater in international law

597 Compilation of treaties and other legal instruments.
598 <https://www.un.org/waterforlifedecade/pdf/groundwaterFao86.pdf>, last accessed 30 January
599 2025
600
601
602 Carvalho, D., Cardoso Pereira, S., Rocha, A., 2020. Future surface temperature changes for the
603 Iberian Peninsula according to EURO-CORDEX climate projections. *Climate Dynamics* 56,
604 123–138. <https://doi.org/10.1007/s00382-020-05472-3>
605
606 Chaminé, H., Afonso, M., Robalo, P., Rodrigues, P., Cortez, C., Monteiro Santos, F., Plancha, J.,
607 Fonseca, P., Gomes, A., Devy-Vareta, N., Marques, J., Lopes, M., Fontes, G., Pires, A.,
608 Rocha, F., 2010. Urban speleology applied to groundwater and geo-engineering studies:
609 underground topographic surveying of the ancient Arca D'Água galleries catchworks (Porto,
610 NW Portugal). *Int J Speleol* 39, 1–14. <https://doi.org/10.5038/1827-806X.39.1.1>
611 Chávez García Silva, R., Reinecke, R., Coptý, N.K., Barry, D.A., Heggy, E., Labat, D., Roggero,
612 P.P., Borchardt, D., Rode, M., Gómez-Hernández, J.J., Jomaa, S., 2024. Multi-decadal
613 groundwater observations reveal surprisingly stable levels in southwestern Europe.
614 *Communications Earth & Environment* 2024 5:1 5, 1–10. [https://doi.org/10.1038/s43247-024-](https://doi.org/10.1038/s43247-024-01554-w)
615 01554-w
616 Chen, C., He, W., Zhou, H., Xue, Y., Zhu, M., 2020. A comparative study among machine learning
617 and numerical models for simulating groundwater dynamics in the Heihe River Basin,
618 northwestern China. *Scientific Reports* 2020 10:1 10, 1–13. [https://doi.org/10.1038/s41598-](https://doi.org/10.1038/s41598-020-60698-9)
619 020-60698-9
620 Reddy, K., Massei, N., Abderrahim Jardani, Henriot, A., Allier, D., Baulon, L., 2022. A wavelet-
621 assisted deep learning approach for simulating groundwater levels affected by low-frequency
622 variability. *The Science of The Total Environment* 865, 161035–161035.
623 <https://doi.org/10.1016/j.scitotenv.2022.161035>
624
625 <https://doi.org/10.1016/J.SCITOTENV.2022.161035>
626 Costa, L.R.D., Hugman, R.T., Stigter, T.Y., Monteiro, J.P., 2021. Predicting the impact of
627 management and climate scenarios on groundwater nitrate concentration trends in southern
628 Portugal. *Hydrogeol J* 29, 2501–2516. <https://doi.org/10.1007/s10040-021-02374-4>
629 Cramer, W., Guiot, J., Fader, M., Garrabou, J., Gattuso, J.P., Iglesias, A., Lange, M.A., Lionello,
630 P., Llasat, M.C., Paz, S., Peñuelas, J., Snoussi, M., Toreti, A., Tsimplis, M.N., Xoplaki, E.,
631 2018. Climate change and interconnected risks to sustainable development in the
632 Mediterranean. *Nature Climate Change* 2018 8:11 8, 972–980. [https://doi.org/10.1038/s41558-](https://doi.org/10.1038/s41558-018-0299-2)
633 018-0299-2
634 Cui, D., Liang, S., Wang, D., 2021. Observed and projected changes in global climate zones
635 based on Köppen climate classification. *Wiley Interdiscip Rev Clim Change* 12, e701.
636 <https://doi.org/10.1002/WCC.701>
637 Cuthbert, M.O., Gleeson, T., Moosdorf, N., Befus, K.M., Schneider, A., Hartmann, J., Lehner, B.,
638 2019. Global patterns and dynamics of climate-groundwater interactions. *Nature Climate*
639 Change 2019 9:2 9, 137–141. <https://doi.org/10.1038/s41558-018-0386-4>
640 Czesla, S., Schröter, S., Schneider, C.P., Huber, K.F., Pfeifer, F., Andreasen, D.T., Zechmeister,
641 M., 2019. PyA: Python astronomy-related packages. *Astrophysics Source Code Library ascl-*
642 1906. <https://github.com/sczesla/PyAstronomy>, last accessed 30 January 2025
643 Davamani, V., John, J.E., Poornachandhra, C., Gopalakrishnan, B., Arulmani, S., Parameswari,
644 E., Santhosh, A., Srinivasulu, A., Lal, A., Naidu, R., 2024. A Critical Review of Climate Change

645 Impacts on Groundwater Resources: A Focus on the Current Status, Future Possibilities, and
646 Role of Simulation Models. *Atmosphere* 15, 122. <https://doi.org/10.3390/atmos15010122>

647 Deines, J.M., Kendall, A.D., Butler, J.J., Hyndman, D.W., 2019. Quantifying irrigation adaptation
648 strategies in response to stakeholder-driven groundwater management in the US High Plains
649 Aquifer. *Environmental Research Letters* 14, 044014. <https://doi.org/10.1088/1748-9326/aafe39>

650

651 Diodato, N., Seim, A., Ljungqvist, F.C., Bellocchi, G., 2024. A millennium-long perspective on
652 recent groundwater changes in the Iberian Peninsula. *Communications Earth & Environment*
653 2024 5:1 5, 1–15. <https://doi.org/10.1038/s43247-024-01396-6>

654 Döll, P., Müller Schmied, H., Schuh, C., Portmann, F.T., Eicker, A., 2014. Global-scale
655 assessment of groundwater depletion and related groundwater abstractions: Combining
656 hydrological modeling with information from well observations and GRACE satellites. *Water*
657 Resour Res 50, 5698–5720. <https://doi.org/10.1002/2014WR015595>

658 Dong, S., Liu, B., Ma, M., Xia, M., Wang, C., 2023. Effects of groundwater level decline to soil and
659 vegetation in arid grassland: A case study of Hulunbuir open pit coal mine. *Environ Geochem*
660 Health 45, 1793–1806. <https://doi.org/10.1007/s10653-022-01292-y>

661 Duan, S., Ullrich, P., Shu, L., 2020. Using Convolutional Neural Networks for Streamflow
662 Projection in California. *Frontiers in Water* 2. <https://doi.org/10.3389/frwa.2020.00028>

663 Earman, S., Dettinger, M., 2011. Potential impacts of climate change on groundwater resources –
664 A global review. *Journal of Water and Climate Change* 2, 213–229.
665 <https://doi.org/10.2166/WCC.2011.034>

666 Eurostat, E.C., Cook, E., 2024. Key figures on the European food chain – 2023 edition.
667 Publications Office of the European Union. <https://doi.org/doi/10.2785/265789>

668 Garrido-Rubio, J., Calera Belmonte, A., Fraile Enguita, L., Arellano Alcázar, I., Belmonte Mancebo,
669 M., Campos Rodríguez, I., Bravo Rubio, R., 2018. Remote sensing-based soil water balance
670 for irrigation water accounting at the Spanish Iberian Peninsula. *Proceedings of the*
671 *International Association of Hydrological Sciences* 380, 29–35. <https://doi.org/10.5194/PIAHS-380-29-2018>

672

673 Gleeson, T., Wada, Y., Bierkens, M.F.P., Van Beek, L.P.H., 2012. Water balance of global
674 aquifers revealed by groundwater footprint. *Nature* 2012 488:7410 488, 197–200.
675 <https://doi.org/10.1038/nature11295>

676 Gómez-Martínez, G., Galiano, L., Rubio, T., Prado-López, C., Darío Redolat, César Paradinas
677 Blázquez, Gaitán, E., María Pedro-Monzonís, Ferriz-Sánchez, S., Soto, M.A., Monjo, R.,
678 Pérez-Martín, M.Á., Llorens, P.A., Cervera, J.M., 2021. Effects of Climate Change on Water
679 Quality in the Jucar River Basin (Spain). *Water* 13, 2424–2424.
680 <https://doi.org/10.3390/w13172424>

681

682 Grantham, T., Christian-Smith, J., Kondolf, G.M., Scheuer, S., 2008. A fresh perspective for
683 managing water in California: Insights from applying the European water framework directive
684 to the Russian River.

685 Emna Guerhazi, Milano, M., Reynard, E., Moncef Zairi, 2018. Impact of climate change and
686 anthropogenic pressure on the groundwater resources in arid environment. *Mitigation and*
687 *Adaptation Strategies for Global Change* 24, 73–92. <https://doi.org/10.1007/s11027-018-9797-9>

688 [9](#)

689

690 Gumuła-Kawęcka, A., Jaworska-Szulc, B., Szymkiewicz, A., Wioletta Gorczewska-Langner,
691 Angulo-Jaramillo, R., Jirka Šimůnek, 2023. Impact of climate change on groundwater recharge
692 in shallow young glacial aquifers in northern Poland. *The Science of The Total Environment*
693 877, 162904–162904. <https://doi.org/10.1016/j.scitotenv.2023.162904>

694
695 Guzman, S.M., Paz, J.O., Tagert, M.L.M., 2017. The Use of NARX Neural Networks to Forecast
696 Daily Groundwater Levels. *Water Resources Management* 31, 1591–1603.
697 <https://doi.org/10.1007/S11269-017-1598-5>
698 Heckert, N.A., Filliben, J.J., Croarkin, C.M., Hembree, B., Guthrie, W.F., Tobias, P., Prinz, J.,
699 2002. Handbook 151: NIST/SEMATECH e-Handbook of Statistical Methods. NIST. URL
700 <https://www.nist.gov/publications/handbook-151-nistsematech-e-handbook-statistical-methods>
701 (accessed 2.3.25).
702
703 Herrera, S., Fernández, J., Gutiérrez, J.M., 2016. Update of the Spain02 gridded observational
704 dataset for EURO-CORDEX evaluation: Assessing the effect of the interpolation methodology.
705 *International Journal of Climatology* 36, 900–908. <https://doi.org/10.1002/JOC.4391>
706 Herrera, S., Margarida Cardoso, R., Matos Soares, P., Espírito-Santo, F., Viterbo, P., Gutiérrez,
707 J.M., 2019. Iberia01: A new gridded dataset of daily precipitation and temperatures over Iberia.
708 *Earth Syst Sci Data* 11, 1947–1956. <https://doi.org/10.5194/ESSD-11-1947-2019>
709 Heudorfer, B., Liesch, T., Broda, S., 2024. On the challenges of global entity-aware deep learning
710 models for groundwater level prediction. *Hydrol Earth Syst Sci* 28, 525–543.
711 <https://doi.org/10.5194/HESS-28-525-2024>
712 Hunkeler, D., Malard, A., Arnoux, M., Jeannin, P., and Brunner, P., 2021. Effect of Climate
713 Change on Groundwater Quantity and Quality in Switzerland. Hydro-CH2018 Project.
714 Comissioned by the Federal Office for the Environment (FOEN), Bern, Switzerland. 80
715 pp. Jacob, D., Elizalde, A., Haensler, A., Hagemann, S., Kumar, P., Ralf Podzun, Rechid, D.,
716 Armelle Reça Remedio, Saeed, F., Sieck, K., Teichmann, C., Wilhelm, C., 2012. Assessing the
717 Transferability of the Regional Climate Model REMO to Different COordinated Regional
718 Climate Downscaling EXperiment (CORDEX) Regions. *Atmosphere* 3, 181–199.
719 <https://doi.org/10.3390/atmos3010181>
720
721 Jan, C.-D., Chen, T.-H., Lo, W.-C., 2007. Effect of rainfall intensity and distribution on groundwater
722 level fluctuations. *Journal of Hydrology* 332, 348–360.
723 <https://doi.org/10.1016/j.jhydrol.2006.07.010>
724
725 Jeong, J., Park, E., 2019. Comparative applications of data-driven models representing water table
726 fluctuations. *Journal of Hydrology* 572, 261–273. <https://doi.org/10.1016/j.jhydrol.2019.02.051>
727
728 Khoso, A.R., Gu, J., Bhutto, S., Muhammad Javed Sheikh, Vighio, K., Arshad Ali Narejo, 2024.
729 Climate change and its impacts in rural areas of Pakistan: A Literature review. *Journal of*
730 *Environmental Science and Economics* 3, 18–26. <https://doi.org/10.56556/jescae.v3i1.731>
731 Leduc, C., Pulido-Bosch, A., Boualem Remini, 2017. Anthropization of groundwater resources in the
732 Mediterranean region: Processes and challenges. *Hydrogeology Journal* 25, 1529–1547.
733 <https://doi.org/10.1007/s10040-017-1572-6>
734 Llamas, M.R., Custodio, E., de la Hera, A., Fornés, J.M., 2015. Groundwater in Spain: Increasing
735 role, evolution, present and future. *Environ Earth Sci* 73, 2567–2578.
736 <https://doi.org/10.1007/S12665-014-4004-0/FIGURES/1>
737 Margat, J., Gun, J. van der, 2013. *Groundwater Around the World: A Geographic Synopsis*. CRC
738 Press. <https://doi.org/10.1201/b13977>
739 Mas-Pla, J., Menció, A., 2019. Groundwater nitrate pollution and climate change: Learnings from a
740 water balance-based analysis of several aquifers in a western Mediterranean region
741 (Catalonia). *Environmental Science and Pollution Research* 26, 2184–2202.
742 <https://doi.org/10.1007/S11356-018-1859-8/TABLES/8>

743 Encarnación Moral-Pajares, María Zozaya-Montes, Gallego-Valero, L., 2024. Globalization Versus
744 Regionalization in Agri-Food Exports from Spain and Portugal. *Agriculture* 14, 963–963.
745 <https://doi.org/10.3390/agriculture14060963>
746

747 Moutahir, H., Bellot, P., Monjo, R., Bellot, J., Garcia, M., Touhami, I., 2017. Likely effects of climate
748 change on groundwater availability in a Mediterranean region of Southeastern Spain. *Hydrol*
749 *Process* 31, 161–176. <https://doi.org/10.1002/HYP.10988>

750 Muthukrishnan, R., Poonkuzhali, G., 2017. A Comprehensive Survey on Outlier Detection Methods.
751 *Journal of Scientific Research* 12, 161–171. <https://doi.org/10.5829/idosi.ajejr.2017.161.171>

752 Müller, J., Park, J., Sahu, R., Varadharajan, C., Arora, B., Faybishenko, B., Agarwal, D., 2021.
753 Surrogate optimization of deep neural networks for groundwater predictions. *Journal of Global*
754 *Optimization* 81, 203–231. <https://doi.org/10.1007/S10898-020-00912-0/FIGURES/10>

755 Neidhardt, H., Shao, W., 2023. Impact of climate change-induced warming on groundwater
756 temperatures and quality. *Applied Water Science* 13. [https://doi.org/10.1007/s13201-023-](https://doi.org/10.1007/s13201-023-02039-5)
757 [02039-5](https://doi.org/10.1007/s13201-023-02039-5)
758

759 Odwori, E.O., 2022. Impact of Temperature Changes on Groundwater Levels in Nzoia River Basin,
760 Kenya. *Asian Journal of Geographical Research* 10–36.
761 <https://doi.org/10.9734/AJGR/2022/V5I1119>

762 Pereira, S.C., Carvalho, D., Rocha, A., 2021. Temperature and Precipitation Extremes over the
763 Iberian Peninsula under Climate Change Scenarios: A Review. *Climate* 9, 139–139.
764 <https://doi.org/10.3390/cli9090139>
765

766 Pinto, C.A., Nadezhdina, N., David, J.S., Kurz-Besson, C., Caldeira, M.C., Henriques, M.O.,
767 Monteiro, F.G., Pereira, J.S., David, T.S., 2014. Transpiration in *Quercus suber* trees under
768 shallow water table conditions: The role of soil and groundwater. *Hydrol Process* 28, 6067–
769 6079. <https://doi.org/10.1002/HYP.10097>

770 Pisani, B., Samper, J., Marques, J.E., 2019. Climate change impact on groundwater resources of
771 a hard rock mountain region (Serra da Estrela, Central Portugal). *Sustain Water Resour*
772 *Manag* 5, 289–304. <https://doi.org/10.1007/S40899-017-0129-0>

773 Ribeiro, L., 2007. Groundwater in the Southern Member States of the European Union: an
774 assessment of current knowledge and future prospects, European Academies' Science
775 Advisory Council. Germany. Retrieved from <https://coilink.org/20.500.12592/5bnjzv> on 03 Feb
776 2025. COI: 20.500.12592/5bnjzv. Rosner, B. (1983). Percentage Points for a Generalized ESD
777 Many-Outlier Procedure. *Technometrics*, 25(2), 165–172.
778 <https://doi.org/10.1080/00401706.1983.10487848> Samper, J., Naves, A., Pisani, B., Dafonte,
779 J., Montenegro, L., Aitor García-Tomillo, 2022. Sustainability of groundwater resources of
780 weathered and fractured schists in the rural areas of Galicia (Spain). *Environmental Earth*
781 *Sciences* 81. <https://doi.org/10.1007/s12665-022-10264-5>
782

783 Scanlon, B.R., Fakhreddine, S., Ashraf Rateb, Graaf, I. de, Famiglietti, J., Gleeson, T., Grafton,
784 R.Q., Jobbagy, E., Kebede, S., Seshagiri Rao Kolusu, Konikow, L.F., Long, D., Mekonnen, M.,
785 Schmied, H.M., Mukherjee, A., MacDonald, A., Reedy, R.C., Shamsudduha, M., Simmons,
786 C.T., Sun, A., 2023. Global water resources and the role of groundwater in a resilient water
787 future. *Nature Reviews Earth & Environment* 4, 87–101. [https://doi.org/10.1038/s43017-022-](https://doi.org/10.1038/s43017-022-00378-6)
788 [00378-6](https://doi.org/10.1038/s43017-022-00378-6)
789

790 Akram Seifi, Ehteram, M., Singh, V.P., Amir Mosavi, 2020. Modeling and Uncertainty Analysis of
791 Groundwater Level Using Six Evolutionary Optimization Algorithms Hybridized with ANFIS,
792 SVM, and ANN. Sustainability 12, 4023–4023. <https://doi.org/10.3390/su12104023>
793

794 Smail, R.A., Pruitt, A.H., Mitchell, P.D., Colquhoun, J.B., 2019. Cumulative deviation from moving
795 mean precipitation as a proxy for groundwater level variation in Wisconsin. J Hydrol X 5,
796 100045. <https://doi.org/10.1016/J.HYDROA.2019.100045>

797 Strada, S., Pozzer, A., Giuliani, G., Coppola, E., Solmon, F., Jiang, X., Guenther, A.,
798 Bourtsoukidis, E., Serça, D., Williams, J., Giorgi, F., 2023. Assessment of isoprene and near-
799 surface ozone sensitivities to water stress over the Euro-Mediterranean region. Atmos Chem
800 Phys 23, 13301–13327. <https://doi.org/10.5194/ACP-23-13301-2023>

801 Taylor, R.G., Scanlon, B., Döll, P., Rodell, M., Beek, R. van, Wada, Y., Laurent Longuevergne,
802 Leblanc, M., Famiglietti, J.S., Edmunds, M., Konikow, L., Green, T.R., Chen, J., Taniguchi, M.,
803 Marc, MacDonald, A., Fan, Y., Maxwell, R.M., Yossi Yechieli, Gurdak, J.J., 2012. Ground
804 water and climate change. Nature Climate Change 3, 322–329.
805 <https://doi.org/10.1038/nclimate1744>
806

807 UN World Water Development Report 2020 [WWW Document], 2020. UN-Water. URL
808 <https://www.unwater.org/publications/un-world-water-development-report-2020> (accessed
809 2.3.25).
810

811 Wunderlich, R.F., Lin, Y.-P., Ansari, A., 2022. Regional Climate Change Effects on the Viticulture
812 in Portugal. Environments 10, 5–5. <https://doi.org/10.3390/environments10010005>
813

814 Wunsch, A., Liesch, T., Broda, S., 2022. Deep learning shows declining groundwater levels in
815 Germany until 2100 due to climate change. Nature Communications 13.
816 <https://doi.org/10.1038/s41467-022-28770-2>
817

818 Wunsch, A., Liesch, T., Broda, S., 2021. Groundwater level forecasting with artificial neural
819 networks: A comparison of long short-term memory (LSTM), convolutional neural networks
820 (CNNs), and non-linear autoregressive networks with exogenous input (NARX). Hydrol Earth
821 Syst Sci 25, 1671–1687. <https://doi.org/10.5194/HESS-25-1671-2021>

822 Wu, W.-Y., Lo, M.-H., Wada, Y., Famiglietti, J.S., Reager, J.T., Yeh, P.J.-F., Agnès Ducharne,
823 Yang, Z.-L., 2020. Divergent effects of climate change on future groundwater availability in key
824 mid-latitude aquifers. Nature Communications 11. <https://doi.org/10.1038/s41467-020-17581-y>
825

826 Yue, S., Wang, C.Y., 2002. Applicability of prewhitening to eliminate the influence of serial
827 correlation on the Mann-Kendall test. Water Resources Research 38.
828 <https://doi.org/10.1029/2001wr000861>
829

830 Zektser, I. & Everett, L., 2004. Groundwater resources of the world and their use, UNESCO:
831 United Nations Educational, Scientific and Cultural Organisation. France. Retrieved from
832 <https://coilink.org/20.500.12592/k0p2q0t> on 03 Feb 2025. COI: 20.500.12592/k0p2q0t. Zhang,
833 A., Winterle, J., Yang, C., 2020. Performance comparison of physical process-based and data-
834 driven models: A case study on the Edwards Aquifer, USA. Hydrogeol J 28, 2025–2037.
835 <https://doi.org/10.1007/S10040-020-02169-Z>

836 Zhou, Y., Wu, J., Gao, X., Guo, W., Chen, W., 2022. Hydrochemical Background Levels and
837 Threshold Values of Phreatic Groundwater in the Greater Xi'an Region, China: Spatiotemporal

838 Distribution, Influencing Factors and Implication to Water Quality Management. Exposure and
839 Health 15, 757–771. <https://doi.org/10.1007/s12403-022-00521-0>
840
841